Acoustoelastic effect in anisotropic layered structures

A. V. Osetrov,* H.-J. Fröhlich, R. Koch, and E. Chilla†
Paul-Drude-Institute for Solid State Electronics, Nanoacoustics Group, Hausvogteiplatz 5-7, D-10117 Berlin, Germany
(Received 24 May 2000; revised manuscript received 10 August 2000)

Mechanical stress alters the velocity of acoustic waves, a phenomenon known as AE (acoustoelastic) effect, which is of particular importance for the wave propagation in layered heterostructures. In order to calculate the AE effect of layered systems in the presence of stress we extended the transfer-matrix method for acoustic wave propagation by considering the change of the density, the influence of residual stress, and the modification of the elastic stiffness tensor by residual strain and by third-order constants. The generalized method is applied to the calculation of the angular dispersion of the AE effect for transverse bulk modes and surface acoustic waves on the Ge(001) crystal cut. The AE effect is found to depend significantly on the propagation direction and can even change sign. The maximum velocity change occurs for transversally polarized waves propagating parallel to the [110] direction. For the layered Ge/Si(001) system the AE effect is investigated for Love modes propagating in the [100] and [110] directions. The AE effect increases rapidly with increasing layer thickness and reaches almost its maximum value when the wave is still penetrating into the unstressed substrate. For higher-order Love modes the increase of the AE effect is even steeper and, furthermore, can reach higher values.

I. INTRODUCTION

The AE (acoustoelastic) effect, i.e., the velocity change of the acoustic waves in the presence of mechanical stress, has been investigated for more than 40 years.[1] AE investigations were mainly stimulated by the interest in the third-order elastic constants and residual stresses in polycrystalline materials, e.g., metal alloys and ceramics.[2–4] So far most of these investigations concentrate on stressed bulk materials.[3–9] Since the stress in bulk materials usually is limited to values of some 100 MPa, the corresponding AE effect is very small and requires high precision acoustic velocity measurements.

In layered systems, on the other hand, considerably higher stresses can occur. Particularly in heteroepitaxy huge stresses in the GPa range usually develop due to the misfit between the lattices of film and substrate. Hence the stress of such films can exceed the tensile strength of bulk materials by about one order of magnitude. For Ge films on Si substrates the lattice misfit is 4.1%. Recent stress investigations of Ge/Si(001) revealed compressive stresses between -2.8 and -5.8 GPa depending on the deposition temperature,[10] in good agreement with the misfit stress calculated by bulk elasticity. For Ge/Si(111) stress values up to -6.7 GPa have been observed.[11] Although these high stresses appear only within a very small thickness range, they can essentially modify local material properties, and in particular the elastic behavior. Therefore acoustic measurements can be utilized to investigate the stress distribution of layered structures.[12]

For the investigation of the AE effect in single-crystalline heterostructures two points have to be considered: (i) Since in surface modes the elastic energy is concentrated close to the surface, they interact more effectively with the stressed layers and are therefore preferable to bulk waves. (ii) For layered structures a variety of additional acoustic modes[13] can exist exhibiting different polarization of the particle displacement vector as well as different acoustic velocities with respect to the propagation direction and operation frequency; hence the AE effect shows an additional frequency dependence as a function of the film thickness and the propagation direction.

In this paper we investigate the AE effect of acoustic waves, in particular SAW's (surface acoustic waves), in stressed systems. In Sec. II the physical model of the residual stresses is outlined on basis of a cubic heterostructure under biaxial and uniaxial stress. In Sec. III the acoustoelastic theory[3] is applied to the SAW propagation in stressed systems. Section IV describes a generalized approach for the calculation of SAW's based on the TMM (transfer-matrix method)[14] which is modified for residual stresses. In Sec. V we apply the modified TMM for acoustic wave propagation in cubic materials. The angular dispersion is calculated for bulk and surface waves. The AE effect in layered systems is discussed in Sec. VI by means of the propagation of Love modes in stressed Ge films on Si(001).

II. PHYSICAL MODEL OF RESIDUAL STRESSES

The calculations are based on the prototype geometry shown in Fig. 1. A stressed layer is deposited onto a substrate. The interface between the layer and the bulk is assumed to be flat, i.e., the rms roughness is much smaller than the acoustic wavelength. This condition is fulfilled for most MBE (molecular-beam epitaxy) grown systems, where the roughness is approximately 1 nm or below. We assume the plane SAW's to propagate parallel to the x_1 axis. The phase velocity of SAW propagation on Si(001) parallel to the [100] direction is $v = 4904.4$ m/s. Hence the flat interface assumption is valid up to very high frequencies.

Due to the misfit the Ge layer is compressed by the epitaxial growth. For our calculations we use the following model geometry of residual stresses and strains. The static stresses and strains can be described by 12 three-dimensional functions $\sigma_{ij}^{(0)}(x_1,x_2,x_3)$ and $u_{ij}^{(0)}(x_1,x_2,x_3)$; $i,j=1,2,3$ with $i \geqslant j$, where $\sigma_{ij}^{(0)}$ is the static stress tensor and $u_{ij}^{(0)}$ is the

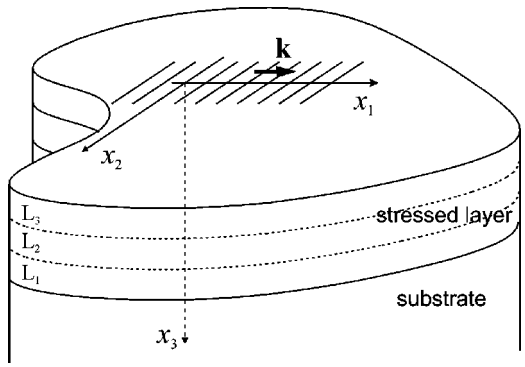

FIG. 1. Schematic illustration of the propagation geometry of a plane acoustic wave with wave vector **k**. The film is divided into sublayers when the stress changes with thickness.

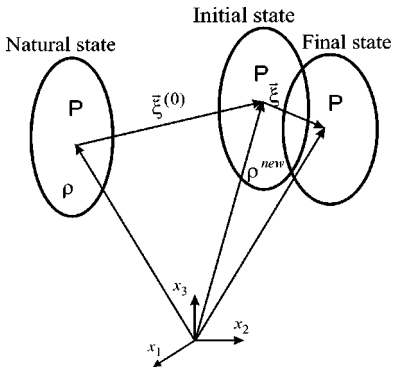

FIG. 2. The natural state of matter changes to the initial state when stresses are applied. The acoustic propagation is studied within the final state.

static strain tensor. The superscript (0) denotes the static behavior where the parameters are independent of time and of SAW propagation. This general description is simplified by several assumptions. First of all we assume that Hooke's law

$$u_{ij}^{(0)} = s_{ijkl}\ \sigma_{kl}^{(0)} \tag{2.1}$$

is fulfilled, where s_{ijkl} are the components of the fourth-order compliance tensor. Hence the number of independent functions $\sigma_{ij}^{(0)}(x_1,x_2,x_3)$; $i,j=1,2,3$; $i \geqslant j$ is reduced to six. Second, we assume a homogeneous lateral stress distribution in the (x_1,x_2) plane, i.e., only the stress value $\sigma_{ij}^{(0)}(x_3)$ changes as a function of the film thickness.

At the interface between the film and the substrate the stress is exclusively determined by the lattice mismatch, no stress components perpendicular to the interface exist:

$$\sigma_{3i}^{(0)}(x_3) = 0. \tag{2.2}$$

For Ge/Si(001) it has been observed that the stress suddenly changes at the different growth stages, directly related to the relief of misfit strain.[10] Such a stress behavior can be described by dividing the film in sublayers (Fig. 1). The properties of the sublayers are determined by the identical material parameters differing only with respect to the three in-plane stress components $\sigma_{11}^{(0)}$, $\sigma_{22}^{(0)}$, $\sigma_{12}^{(0)}$. In this particular case the static boundary conditions between the sublayers are automatically fulfilled since the normal stress components are equal to zero [see Eq. (2.2)]. In principle, any stress profile within a layer can be simulated by constant stresses when the layer is splitted into a number of sublayers with gradually differing stresses. In Sec. IV we will explain how the transfer-matrix methods is particularly useful for the description of stressed multilayer systems.

In cubic heterostructures usually the lateral stress distribution is biaxial or uniaxial. For the Ge/Si(001) layered system the stress distribution is biaxial. If we assume $\sigma_{11}^{(0)} = \sigma_{22}^{(0)} = \sigma$, $\sigma_{12}^{(0)} = 0$, Eqs. (2.1) and (2.2) give $\sigma_{3i}^{(0)} = 0$ and $u_{11}^{(0)} = u_{22}^{(0)} \neq 0$, $u_{33}^{(0)} \neq 0$, $u_{ij}^{(0)} = 0$ for $i \neq j$, respectively. Hence one independent parameter σ for description of the residual stress is left and only axial static stresses and strains exist. However, the expressions derived further can also be used for the uniaxial stress model in cubic materials, where $\sigma_{11}^{(0)} = \sigma$, $\sigma_{22}^{(0)} = \sigma_{12}^{(0)} = 0$, and $u_{11}^{(0)} \neq 0$, $u_{22}^{(0)} = u_{33}^{(0)} \neq 0$, $u_{ij}^{(0)} = 0 (i \neq j)$ is valid.

III. ACOUSTIC WAVES IN STRESSED HETEROSTRUCTURES

In the theory of acoustoelasticity the acoustic propagation under residual stresses is commonly investigated in a prestressed body, the so-called initial state.[3] The original state of the body free of stresses and strains is the natural state (Fig. 2). When the wave motion is superposed to the initial state the body is deformed to the final state. The problem of wave propagation under residual stresses is nonlinear. Therefore the Lagrangian description for the particle motion in space is preferable to the Eulerian. As acoustic parameters we use the displacement vector ξ_i, the strain tensor u_{ij}, and the stress tensor σ_{ij}. These parameters are determined by the difference between the final state displacement and the static displacement, the final and static strain, the second Piola-Kirchhoff stress tensor, and $\sigma_{ij}^{(0)}$. The following assumptions[3] are made: (i) The predeformation is static and the body is at equilibrium in the initial state. (ii) The superposed dynamic motion (responsible for wave propagation) is small. (iii) In the natural state the body is homogeneous but anisotropic. (iv) The process of deformation is either isentropic or isothermal. (v) The body is hyperelastic. With these assumptions the equation of motion becomes[3]

$$\frac{\partial}{\partial x_j}\left[\sigma_{ij} + \sigma_{jk}^{(0)}\frac{\partial \xi_i}{\partial x_k}\right] = \rho^{new}\frac{\partial^2 \xi_i}{\partial t^2}, \tag{3.1}$$

where ρ^{new} is the density after static strains,

$$\rho^{new} \approx \rho(1-\Delta u^{(0)}), \tag{3.2}$$

$$\Delta u^{(0)} = u_{11}^{(0)} + u_{22}^{(0)} + u_{33}^{(0)} = \frac{\partial \xi_1^{(0)}}{\partial x_1} + \frac{\partial \xi_2^{(0)}}{\partial x_2} + \frac{\partial \xi_3^{(0)}}{\partial x_3}, \tag{3.3}$$

ρ is the density of the unstressed material and t is the time, respectively. Furthermore Hooke's law can be written as $\sigma_{ij} = C_{ijkl}u_{kl}$ or

$$\sigma_{ij}=C_{ijkl}\frac{\partial \xi_k}{\partial x_l}, \tag{3.4}$$

where C_{ijkl} are the modified second order stiffness moduli (fourth-order tensor),

$$C_{ijkl}=c_{ijkl}(1-\Delta u^{(0)})+c_{ijklmn}u^{(0)}_{mn}+c_{mjkl}\frac{\partial \xi^{(0)}_i}{\partial x_m}+c_{imkl}\frac{\partial \xi^{(0)}_j}{\partial x_m}+c_{jiml}\frac{\partial \xi^{(0)}_k}{\partial x_m}+c_{ijkm}\frac{\partial \xi^{(0)}_l}{\partial x_m}, \tag{3.5}$$

and c_{ijkl} are the second-order stiffness moduli (fourth-order tensor), c_{ijklmn} are the third-order stiffness moduli (sixth-order tensor), respectively. For arbitrary materials c_{ijklmn} have 56 independent coefficients. In case of cubic materials only six independent moduli are left.[18] In Eqs. (3.1)–(3.5) and later Cartesian coordinates x_i refer to the position of a mass element in the initial state.

Expressions (3.1)–(3.5) represent the total system of equations for the wave propagation in a stressed body, containing nine variables (six stress components σ_{ij} and three displacement components ξ_i) and nine equations [three equations of motion (3.1) and six equations derived from Hooke's law (3.4)]. The main deviations within the system of equations with respect to an unstressed body refer to: (i) a modified density ρ^{new} instead of ρ in the equations of motion (3.1); (ii) a modified stiffness tensor C_{ijkl} instead of c_{ijkl} in Hooke's law (3.4); (iii) an additional term $\partial/\partial x_j[\sigma^{(0)}_{jk}(\partial \xi_i/\partial x_k)]$ within the new equations of motion (3.1). The modified density as well as the stiffness tensor do not alter the main structure of the Eqs. (3.1) and (3.4), because both ρ^{new} and C_{ijkl} do not depend on the coordinates within each sublayer. Thus the layer properties change abruptly at the interface. However, assumption (iii) has serious consequences for the solution of the problem. We shall discuss this in detail in Sec. IV. Here we first rewrite Eqs. (3.1) and (3.5) for our model.

Assuming plane-wave propagation perpendicular to x_2, i.e., $\partial \xi_i/\partial x_2=0$, homogenous static stresses within the sublayer, i.e., $\sigma^{(0)}_{ij}(x_1,x_2,x_3)=\sigma^{(0)}_{ij}$, and the vanishing of the transverse shear stress at the free surface [see Eq. (2.2)], Eq. (3.1) becomes

$$\frac{\partial \sigma_{ij}}{\partial x_j}+\sigma^{(0)}_{11}\frac{\partial^2 \xi_i}{\partial x_1^2}=\rho^{new}\ \frac{\partial^2 \xi_i}{\partial t^2}. \tag{3.6}$$

It depends only on the diagonal static stress in the direction of the wave propagation. In the case of axial static stresses and strains expression (3.5) can be represented as

$$C_{ijkl}=c_{ijkl}(1+u^{(0)}_{ii}+u^{(0)}_{jj}+u^{(0)}_{kk}+u^{(0)}_{ll}-u^{(0)}_{11}-u^{(0)}_{22}-u^{(0)}_{33})+c_{ijklmn}u^{(0)}_{mn}. \tag{3.7}$$

The boundary conditions for the wave motion at the interface between the layers I and II are determined by the continuous particle displacement

$$\xi^{(I)}_i|_S=\xi^{(II)}_i|_S \tag{3.8}$$

and continuous forces

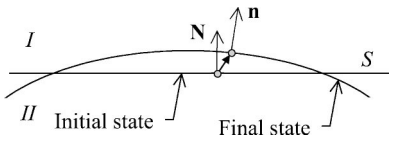

FIG. 3. Schematic illustration of the transformation of the boundary condition from the initial state with normal **N** and final state with normal **n** at the interface S between layer I and substrate II.

$$\left[(\sigma^{(0,I)}_{ij}+\sigma^{(I)}_{ij})+(\sigma^{(0,I)}_{kj}+\sigma^{(I)}_{kj})\frac{\partial \xi^{(I)}_j}{\partial x_k}\right]N_j\Big|_S=\left[(\sigma^{(0,II)}_{ij}+\sigma^{(II)}_{ij})+(\sigma^{(0,II)}_{kj}+\sigma^{(II)}_{kj})\frac{\partial \xi^{(II)}_j}{\partial x_k}\right]N_j\Big|_S; \tag{3.9}$$

superscripts (I), (II), denote the layer numbers and S is the interface surface, respectively. $\mathbf{N}=N_j$ is the normal between layers at the initial state (Fig. 3). On each side of Eq. (3.9) the second terms accounts for stress transformation from the initial state (with normal **N**) to the final state (with normal **n**).

Neglecting the term $\sigma^{(I,II)}_{kj}(\partial \xi_i/\partial x_k)$, considering $\mathbf{N}=(0,0,1)$ and taking into account Eqs. (2.2) we obtain for Eq. (3.9)

$$\sigma^{(I)}_{i3}|_S=\sigma^{(II)}_{i3}|_S. \tag{3.10}$$

Expression (3.10) is similar for the wave propagation without static stresses. For the free surface, i.e., the surface of the upper layer, $\sigma_{i3}|_S=0$.

IV. TRANSFER-MATRIX METHOD FOR SAW PROPAGATION UNDER RESIDUAL STRESS

For the calculation of SAW's in layered structures mainly two approaches have been applied so far. In the partial wave method an exponential ansatz is assumed for the acoustic displacements in the substrate as well as in each layer in both x_1 and x_3 directions. Then a total system of coupled nonlinear equation can be formulated when the boundary conditions are taken into account. This approach has also been extended to stressed material regarding static stresses only.[19] However, for multilayered systems the coefficient determinant for the boundary conditions is multidimensional and can influence the stability of the numerical solution significantly. This problem can be overcome by applying the TMM (transfer-matrix method) for acoustic wave propagation.[14,15] The TMM is based on a complete set of independent parameters that are continuous at the interfaces. Then the boundary conditions are automatically fulfilled. Hence the TMM is particularly useful for multilayered heterostructures. Here we will formulate the TMM for SAW propagation under residual stresses.

According to Fahmy and Adler[14] we represent the stress and the displacement by the ansatz

$$\sigma_{ij}(x_1,x_3)=\hat{\sigma}_{ij}(x_3)e^{J(\omega t-kx_1)}, \tag{4.1}$$

$$\xi_i(x_1,x_3)=\hat{\xi}_i(x_3)e^{J(\omega t-kx_1)}, \tag{4.2}$$

where $\hat{\sigma}_{ij}(x_3)$ and $\hat{\xi}_i(x_3)$ describe the depth dependence for the total system, $k=\omega/v$ is the wave number, $\omega=2\pi f$ the angular frequency, and v is the phase velocity. Insertion of Eqs. (4.1) and (4.2) into the equation of motion (3.1) gives

$$\frac{d\hat{\sigma}_{i3}}{dx_3}=-(\rho^{new}\omega^2-\sigma_{11}^{(0)}k^2)\xi_i+Jk\hat{\sigma}_{i1} \tag{4.3}$$

and into Hooke's law (3.4) gives

$$\hat{\sigma}_{i1}=-JkC_{i1k1}\hat{\xi}_k+C_{i1k3}\frac{d\hat{\xi}_k}{dx_3},$$

$$\hat{\sigma}_{i3}=-JkC_{i3k1}\hat{\xi}_k+C_{i3k3}\frac{d\hat{\xi}_k}{dx_3}. \tag{4.4}$$

After substitution of $\hat{\sigma}_{i1}$ from Eq. (4.4) in Eq. (4.3) we receive the following system of six differential equations for $\hat{\sigma}_{i3}$ and $\hat{\xi}_i$

$$\frac{d\hat{\sigma}_{i3}}{dx_3}=-\omega^2\left[\rho^{new}\delta_{ik}-\frac{1}{v^2}(C_{i1k1}+\sigma_{11}^{(0)}\delta_{ik})\right]\hat{\xi}_k+JkC_{i1k3}\frac{d\hat{\xi}_k}{dx_3}, \tag{4.5}$$

$$C_{i3k3}\frac{d\hat{\xi}_k}{dx_3}=JkC_{i3k1}\hat{\xi}_k+\hat{\sigma}_{i3},$$

with δ_{ik} being the Kronecker-symbol. Since the solution of the system of equations has to be continuous at the interfaces we construct according to the boundary conditions (3.8) and (3.10) a vector

$$\mathbf{\Gamma}=[\hat{\sigma}_{13}\hat{\sigma}_{23}\hat{\sigma}_{33}J\omega\hat{\xi}_1J\omega\hat{\xi}_2J\omega\hat{\xi}_3]^T \tag{4.6}$$

of the displacement components $\hat{\xi}_i$ and three components of stress tensor $\hat{\sigma}_{i3}$, where T denotes the transpose of the matrix. Then Eq. (4.5) can be written in the matrix representation

$$\frac{d\mathbf{\Gamma}}{dx_3}=J\omega\mathbf{F}(v)\mathbf{\Gamma}, \tag{4.7}$$

where

$$\mathbf{F}(v)=\frac{1}{v^2}\begin{bmatrix}v\mathbf{B}\mathbf{C}^{-1} & v^2\rho^{new}\mathbf{I}-\mathbf{A}+\mathbf{B}\mathbf{C}^{-1}\mathbf{B}^T\\ v^2\mathbf{C}^{-1} & v\mathbf{C}^{-1}\mathbf{B}^T\end{bmatrix}, \tag{4.8}$$

with

$$\mathbf{A}=C_{i1k1}+\sigma_{11}^{(0)}\delta_{ik},\quad \mathbf{B}=C_{i1k3},$$

$$\mathbf{B}^T=C_{i3k1},\quad \mathbf{C}=C_{i3k3}, \tag{4.9}$$

I being the identity matrix and

$$\mathbf{A}=\begin{bmatrix}C_{11}+\sigma_1^{(0)} & C_{16} & C_{15}\\ C_{16} & C_{66}+\sigma_1^{(0)} & C_{56}\\ C_{15} & C_{56} & C_{55}+\sigma_1^{(0)}\end{bmatrix}, \tag{4.10}$$

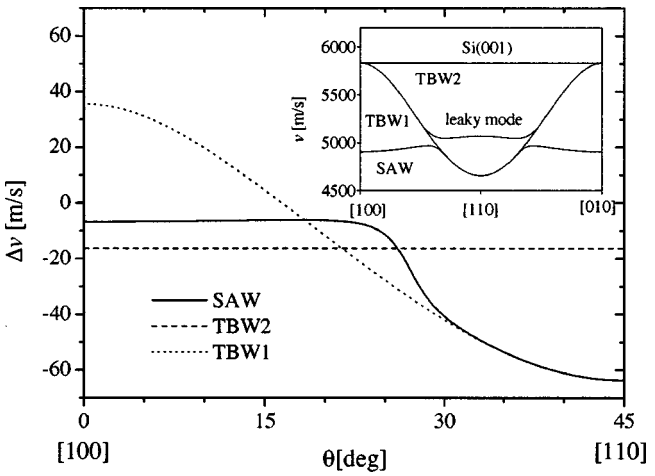

FIG. 4. Azimuthal dependence of the phase velocity shift Δv for Ge(001) for the SAW (solid), the quasitransverse (dotted), and the transverse bulk waves (dashed) under biaxial stress of -1 GPa. The inset shows the azimuthal phase velocity dispersion of the Si(001) cut for the SAW, the leaky SAW, as well as the transverse bulk wave (TBW2) and the quasitransverse bulk wave (TBW1).

$$\mathbf{B}=\begin{bmatrix}C_{15} & C_{14} & C_{13}\\ C_{56} & C_{46} & C_{36}\\ C_{55} & C_{45} & C_{35}\end{bmatrix},\quad \mathbf{C}=\begin{bmatrix}C_{55} & C_{45} & C_{35}\\ C_{45} & C_{44} & C_{34}\\ C_{35} & C_{34} & C_{33}\end{bmatrix},$$

according to Voigt notation. Expressions (4.6)–(4.7) have the same character as for the transfer-matrix approach without static stresses and strains. Hence the numerical procedure for the solution is similar to the unstressed body. For $\sigma_{11}^{(0)}=0$, $\rho^{new}=\rho$ and $C_{ijkl}=c_{ijkl}$ the solution for the wave propagation in the unstressed body can be found.

V. ACOUSTOELASTIC EFFECT IN SEMI-INFINITE CUBIC MATERIALS

The calculation of acoustic waves in a homogeneous half-space has already been treated in the earlier literature. The isotropic case is addressed, e.g., in the review of Pao *et al.*[3] The first calculation of the influence of stress on SAW's was carried out by Hayes and Rivlin.[5] Hirao *et al.*[6] discussed stress variations as a function of penetration depth. Mase and Johnson[7] presented calculations for SAW in homogeneously stressed half space. In this section we apply the generalized transfer-matrix method for the calculation of acoustic waves in semi-infinite cubic substrates. It is well known that in cubic materials the two orthogonally polarized transverse bulk waves propagating parallel to the [100] crystal axis have the same phase velocity. When the propagation direction is rotated in the (001) plane the phase velocity of the transverse bulk waves split off and one mode becomes quasitransverse while the other still stays pure transversally polarized. The quasitransverse wave exhibits a large angular dispersion while the velocity of the pure transverse wave is constant over the total angular range. The SAW on the (001) cut in the [100] direction is polarized within the sagittal plane, i.e., the plane determined by the normal of the plane and the wave propagation direction, hence it is a Rayleigh-type wave. Also the SAW shows an angular velocity dispersion (see inset in Fig. 4). When it approaches the [110] di-

TABLE I. Elastic constants c_{ij} [GPa] and density $\rho\,[kg/m^3]$ of Si and Ge (Ref. 18).

	c_{11}	c_{12}	c_{44}	ρ
Si	165	64	79.2	2329
Ge	129	48	67.1	5323.4

rection it changes the polarization from sagittal to transverse and converts into the quasitransverse bulk wave. However, for the [110] direction also a true sagittally polarized SAW exists. This wave appears from the leaky branch and has been discussed in detail by Farnell.[20]

Table I lists elastic constants; in Table II the respective phase velocities of Si and Ge are plotted, which are calculated from the data of Table I. Here we are mainly interested in the mode behavior as a function of the residual stress. In particular, we will discuss the influence of the stress on the SAW and the transverse modes for very thick Ge layers approximated by a semi-infinite model, where the wave properties are determined by the layer properties only. The velocities are calculated for the data from Tables I and III. Figure 4 shows the angular dependence of the AE effect $\Delta v(\sigma)=v(\sigma)-v(0)$ at a biaxial stress of -1 GPa for Ge(001); $v(\sigma)$ and $v(0)$ are the phase velocities with and without stress, respectively. Obviously the AE effect depends on the propagation direction. While the AE effect is small and constant for the pure transverse wave, the change of the velocity is very high for the quasitransverse mode in the symmetry directions and moreover changes even sign. The SAW propagation parallel to [100] is only slightly influenced by stress. However, when the polarization of the SAW changes to transverse, the wave is increasingly influenced by stress. The maximum change of about -65 m/s is calculated near the [110] direction, where the SAW is polarized almost transversally.

In a first approximation the dependence of the phase velocity on the stress is linear. Then the relative velocity shift $\delta v(\sigma)=\Delta v(\sigma)[-1GPa/\sigma]-\Delta v(-1GPa)$ can be calculated. As shown in Fig. 5 for the quasitransversal bulk wave and the SAW the values of $\delta v(\sigma)$ are quite small although the stress changes by more then one order of magnitude. Only in the small angular range at about 25° a more drastic change of δv of the SAW is observed. For the pure transverse wave (not shown in Fig. 5) the relative velocity shift is independent on the azimuthal propagation direction, i.e., $\delta v=-0.08$ m/s and $\delta v=0.41$ m/s for -0.2 GPa and -5 GPa, respectively. The steep variation for the SAW at about 25° results from the rapid increase of the AE effect in this angular region (Fig. 4). When the stress increases δv switches from positive to negative. By using δv from Fig. 5 and Δv from Fig. 4 the total AE effect can be estimated for different stresses and azimuthal propagation directions. For a typical biaxial stress of -0.2 GPa in thick films the AE effect for SAW propagation near the [110] direction is about -12 m/s. This velocity change is indeed remarkable and accessible to measurement by high accuracy acoustic methods.

TABLE II. Calculated sound velocities on Si(001) and Ge(001).

Propagation direction	Wave type	Phase velocity [m/s] Si(001)	Ge(001)
[100]	transverse wave	5831.5	3550.3
[100]	SAW, sagittal polarization	4904.4	2933.7
[110]	transverse wave	4656.5	2758.2

TABLE III. 3rd-order elastic constants c_{ijk}[GPa] of Ge (Ref. 18).

c_{111}	c_{112}	c_{123}	c_{144}	c_{155}	c_{456}
-720	-380	-30	-10	-305	-45

VI. LOVE WAVES IN STRESSED GE/SI(001)

Although the general behavior of Ge and Si is similar, the acoustic modes of Ge are considerably slower (cf. Table II). Hence when a Ge layer is deposited on a Si substrate the phase velocity of all surface modes decreases depending on both the layer thickness h and the frequency f of the wave. For layered systems, where the film slows down the wave propagation, new transversally polarized surface modes, so-called Love modes, appear.

For a thin Ge film the velocity of this mode is close to the bulk wave of the Si substrate. With increasing the thickness the velocity decreases until it converges to the velocity of the bulk wave of Ge (cf. Table II). Additionally higher order modes set in when fh reach certain threshold values. Figure 6 shows the fh dispersion of the phase velocity for the fundamental and the higher-order Love modes for the [100] direction calculated by the TMM. For the [110] direction the Love waves sets in from the quasitransverse wave.

For a homogeneously stressed layer on a surface of a semi-infinite elastic medium Maradudin and Mayer[16] have analytically derived the velocity change in case of the thin film approximation. Here the acoustic wavelength is much larger than the film thickness and the displacement field can be considered to vary only slightly on a length scale given by the film thickness.[17] For thicker films, however, the displace-

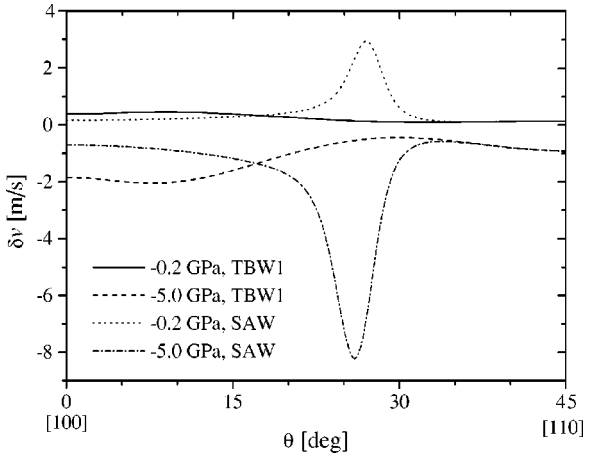

FIG. 5. Azimuthal dependence of the relative velocity change δv for SAW and quasitransverse bulk wave propagation in Ge(001) at biaxial stresses of -0.2 GPa and -5 GPa compared to the values at -1 GPa.

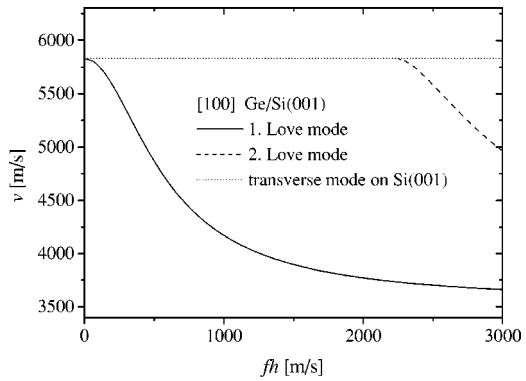

FIG. 6. Phase velocity of the fundamental (solid) and the first order (dashed) Love mode in the Ge/Si(001) layered system for wave propagation parallel to the [100] axis as function of the frequency-thickness product fh. The Love wave sets in at the velocity of the transverse bulk wave (dotted) of Si(001).

ment component may change significantly also within the film. Then the AE effect depends also on the penetration depth of the wave. In particular, the AE effect is expected to be maximum when wavelength is much smaller than the thickness of the layer, because then the wave is completely localized within the stressed material. Hence measurements at high frequency, i.e., small wavelength, are preferred for stress investigation of thin films.

For Love waves on Ge/Si(001) the AE effect indeed approaches its maximum value when fh is infinite (see Fig. 7). It is interesting, however, that the AE effect approaches its maximum value rapidly. For an operation frequency of 10 GHz and a layer thickness of about 50 nm the velocity shift for the fundamental Love mode parallel to [110] is about -45 m/s at stress of -1 GPa. According to $\delta v(\sigma)$ the velocity shift for this structure is about -10 m/s for -0.2 GPa. For the higher-order modes the AE effect increases much more rapidly than for the fundamental mode and can even reach higher values. Furthermore, in agreement with the behavior of the quasitransverse bulk wave the AE effect changes sign when the Love mode propagation turns from the [100] to the [110] direction.

In Fig. 8 the velocity change is calculated for a Love

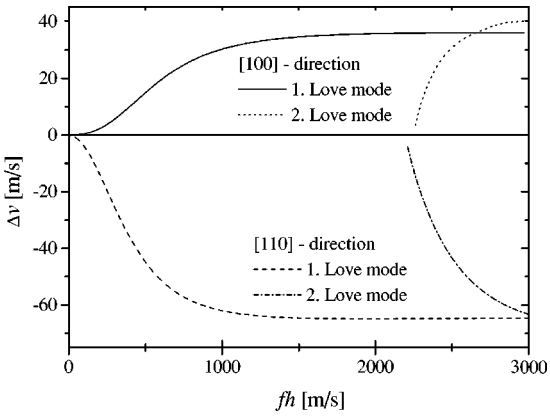

FIG. 7. Phase velocity shift Δv of the fundamental and higher-order Love waves propagating parallel to the [100] and [110] direction for -1 GPa biaxially stressed Ge films on Si(001) as function of the frequency-thickness product fh.

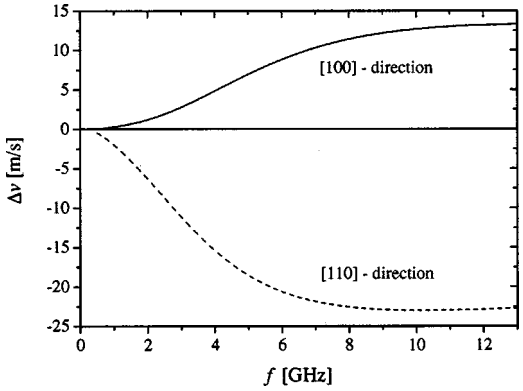

FIG. 8. Dependence of the phase velocity change Δv on the frequency f of the Love mode in [100] and [110] direction for a inhomogeneously stressed Ge/Si(001) system (see text).

wave in a inhomogeneously stressed Ge films on Si(001) reported recently.[10] The Ge film consists of three sublayers of thicknesses of 1, 60, and 40 nm exhibiting biaxial stress of 5, 0.6, and 0.13 GPa, respectively. For this system the maximum velocity shift of the Love mode is about 13 m/s in the [100] direction and -23 m/s in the [110] direction. However, the AE effect increases rapidly with frequency and reaches almost the maximum well below 10 GHz. Figure 9 displays the penetration dependence of the particle displacement (i.e., the shear-horizontal component ξ_2) into the material (i.e., along x_3). The oscillation is increasingly localized near the surface when the frequency increases. Below 1 GHz the oscillation amplitude within the layer is nearly constant. For higher frequencies, however, the amplitude changes drastically already within the film. Although at 10 GHz the velocity shift is close to its maximum value (cf. Fig. 8) the wave still penetrates considerably into the unstressed Si substrate.

VII. CONCLUSION

We adapted the TMM (transfer-matrix method)[14] to calculate the acoustic wave propagation in layered systems un-

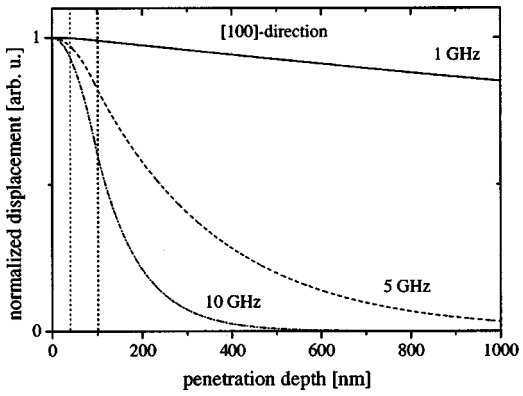

FIG. 9. Dependence of the particle displacement with respect to the penetration depth into the inhomogeneously stressed Ge/Si(001) system for Love mode propagation in [100] direction at $f=1$ GHz (solid), 5 GHz (dashed), and 10 GHz (dash dotted). The three differently stressed Ge layers (1 nm, 5 GPa; 60 nm, 0.6 GPa; 40 nm, 0.13 GPa) are indicated by dotted vertical lines. Notice that at higher frequencies the wave is increasingly localized within the Ge film, although the velocity shift is close to its maximum value (cf. Fig. 8).

der residual stress by including also the change of the density, the influence of the residual stress and the modification of the elastic stiffness tensor by residual strain and by third-order stiffness constants. This generalized method is particularly useful for investigations of surface guided acoustic waves in multilayered systems with vertically inhomogenous stress distribution. We calculated bulk and surface acoustic modes for biaxially stressed Ge(001). The value of the AE effect depends significantly on the propagation direction and can even change sign. The maximum velocity change is found for the transverse wave in the [110] direction. The SAW is very sensitive to stress at a rotation angle of about 25° from the [100] axis. For Love waves in Ge/Si(001) the AE effect is maximum for high frequencies, i.e., small wavelengths, and thick layers. However, the AE effect increases very rapidly and reaches almost the maximum value even when the wave is still deeply penetrating into the unstressed substrate. For higher-order Love modes the increase of the AE effect is even steeper and can reach larger values compared to the fundamental mode. In agreement with the stress behavior of the quasitransverse wave the AE effect for Love waves changes sign when the propagation is turned from the [100] to the [110] direction. Further calculation will be carried out for Rayleigh waves multilayered stressed systems and piezoelectric materials.

ACKNOWLEDGMENTS

The authors thank Zuliang Yu for helpful discussions. One of us (E.C.) is thankful to M. Konagai for the support during his stay at the Tokyo Institute of Technology.

*Permanent address: Electroacoustics and Ultrasonics Department, St. Petersburg State Electrotechnical University, Prof. Popov 5, 197376 St. Petersburg, Russia.

†Corresponding author. Email address: e.chilla@pdi-berlin.de

[1] D. S. Hughes and J. L. Kelly, Phys. Rev. **92**, 1145 (1953).

[2] R. N. Thurston and K. Brugger, Phys. Rev. **133**, A1604 (1964).

[3] Y. H. Pao, W. Sachse, and H. Fukuoka, in *Physical Acoustic*, edited by W. P. Mason and R. N. Thurston (Academic, New York, 1984), Vo. 17, pp. 62–143.

[4] T. Berruti, M. M. Gola, and G. A. D. Briggs, J. Acoust. Soc. Am. **103**, 1370 (1998).

[5] M. Hayes and R. S. Rivlin, Arch. Ration. Mech. Anal. **8**, 358 (1961).

[6] M. Hirao, H. Fukuoka, and K. Hori, J. Appl. Mech. **48**, 119 (1981).

[7] G. T. Mase and G. C. Johnson, J. Appl. Mech. **54**, 127 (1987).

[8] A. D. Degtyar and S. I. Rokhlin, J. Appl. Phys. **78**, 1547 (1995).

[9] Marc Duquennoy, Mohammadi Ouaftouh, Mohamed Ourak, and Wei-Jiang Xu, J. Appl. Phys. **86**, 2490 (1999).

[10] G. Wedler, J. Walz, T. Hesjedal, E. Chilla, and R. Koch, Phys. Rev. Lett. **80**, 2382 (1998).

[11] J. Walz, A. Greuer, G. Wedler, T. Hesjedal, E. Chilla, and R. Koch, Appl. Phys. Lett. **73**, 2579 (1998).

[12] We note that the stress is deduced from the wave velocity by solving the inverse problem of the wave propagation. Since the inverse problem is nonlinear, precise knowledge of a variety of material parameters is required. The error usually is minimized by analyzing the behavior of different acoustic modes in various propagation geometries.

[13] G. W. Farnell and E. L. Adler, in *Physical Acoustic*, edited by W. P. Mason and R. N. Thurston (Academic, New York, 1972), Vol. 9, pp. 35–127.

[14] A. H. Fahmy and E. L. Adler, Appl. Phys. Lett. **22**, 495 (1973).

[15] E. L. Adler, IEEE Trans. Ultrason. Ferroelectr. Freq. Control **41**, 876 (1994).

[16] A. A. Maradudin and A. P. Mayer, in *Nonlinear Waves in Solid State Physics*, Vol. 247 of *NATO Advanced Study Institute, Series B: Physics*, edited by A. D. Boardman, T. Twardowski, and M. Bartolotti (Plenum Press, New York, 1990), p. 113–161.

[17] B. A. Auld, in *Acoustic Fields and Waves in Solids*, 2nd edition (Robert E. Krieger Publishing, Malabar, 1990), Vol. II.

[18] R. F. S. Hearmon, in *Crystal and Solid State Physics*, Landolt-Börnstein, New Series, Group III, Vol. 11 (Springer, Berlin, 1979), pp. 1–286.

[19] Z. Sklar, P. Mutti, N. C. Stoodley, and G. A. D. Briggs, in *Advances in Acoustic Microscopy*, edited by G. A. D. Briggs (Plenum Press, New York, 1995), Vol. 1, pp. 209–247.

[20] G. W. Farnell, in *Physical Acoustic*, edited by W. P. Mason and R. N. Thurston (Academic, New York, 1970), pp. 109–166.